ACS APPLIED MATERIALS & INTERFACES

Research Article

www.acsami.org

Site-Selective Growth of Patterned Silver Grid Networks as Flexible Transparent Conductive Film by Using Poly(dopamine) at Room Temperature

Yunxia Jin, Yuanrong Cheng, Dunying Deng, Chengjie Jiang, Tianke Qi, Donglun Yang, and Fei Xiao*

Department of Materials Science, Fudan University, 220 Handan Road, Shanghai 200433, China

ABSTRACT: Metal transparent conductive films (TCFs) have received increasing attention in various flexible electronics. However, there are two crucial issues that need to be addressed: (1) strong adhesion between metal TCFs and the flexible substrates and (2) high conductivity with short treatment time and low process temperature, simultaneous with high transparency. In this paper, a site-selective electroless plating combination with poly(dopamine) modification is demonstrated to fabricate a new high performance transparent conductor composed of a periodic two-dimensional silver network on a heat sensitive flexible substrate at room temperature. The TCF reveals an extremely high ratio of DC to optical conductivity (σ_{DC}/σ_{Op}) value in the range of 350−1000 for various fabricated silver grid films. It also exhibits particularly strong adhesion, which can resist ultrasonic treatment in water or organic solvent for several hours. Its reliability (stable for at least 1440 h during 85 °C/85% RH aging) meets the essential requirements for microelectronic applications. Using this method, we obtain silver grid film on a flexible polyethylene terephthalate substrate with optical transmittance of 91% and sheet resistance of 8 Ohm sq^{-1}, which is comparable to or better than the commercially available indium tin oxide.

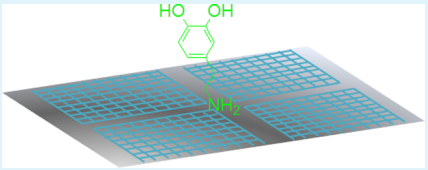

KEYWORDS: *flexible electronics, surface modification, silver grid, site-selection, patterning*

INTRODUCTION

Transparent conductive films (TCFs) are widely used as electrodes in many optoelectronic devices, such as liquid crystal displays, organic light emitting diodes, organic solar cells, touch panels, and electromagnetic interference shielding materials.[1−6] However, two crucial issues should be addressed: (1) strong adhesion between TCFs and the flexible substrates and (2) high conductivity and high transparency with a short and low temperature fabrication process. Carbon nanotubes (CNTs) and, more recently, graphene films have been successfully developed as TCFs and have attracted significant interest,[7−9] but the conductivity is typically not comparable to the commercial indium tin oxide (ITO). The reported best figure-of-merit conductivity−transmittance, the ratio of DC to optical conductivity (σ_{DC}/σ_{Op}), is 25 for CNTs[10] and 113 for graphene.[8] For the application of solar cells and OLEDs, the optical transmittance (T) and sheet resistance (R_s) typically need to be ≥90% and ≤10 Ohm sq^{-1}, respectively, meaning a value of σ_{DC}/σ_{Op} = 350.[1] A lower sheet resistance can be obtained with silver nanowires (AgNWs) because the conductivity of silver is much higher than that of carbon single-walled nanotubes.[11−14] The maximum value of σ_{DC}/σ_{Op} is 500, due to 32% transmittance and 0.5 Ohm sq^{-1} sheet resistance,[11] but at high transmittance, the value is still much less than 350. Possible reasons for the limited performance of AgNW films include the low aspect ratio,[15] poor uniform deposition on the substrate,[16] and the relatively high contact resistance due to the surfactant molecules (e.g., polyvinylpyrrolidone) coating on the surfaces of AgNWs. High optical transmittance and high electrical conductivity could be achieved with the periodic metallic structure benefiting from the much lower contact resistance of the well-connected metallic grids.

Various fabricating methods have been reported. Kang and Guo fabricated such metal grids on rigid substrates via nanoimprinting lithography, and demonstrated the applications in solar cells and OLEDs.[15] Inkjet printing, screen printing, transfer printing et al. were also reported to prepare the metal grids and were successfully used in solar cells.[16−18] However, they suffer from the micrometer-scale thickness leading to extreme surface roughness of the substrate, high temperature postprinting sintering, or poor adhesion. The best value of σ_{DC}/σ_{Op} for metallic grids is 237, which has not exploited the strength of the periodic metallic structure.[18] Besides, regardless of the TCF type, CNTs, graphene, AgNWs, or metal grids, most research is concentrated on improving conductivity and transparency, with very little focused on the adhesive performance and almost none working on the long-term reliability, which are both issues that must be resolved before industrial application. Thus, a flexible TCF exhibiting a comparable value of σ_{DC}/σ_{Op} to ITO, qualified adhesive, and reliable performance to meet the commercial requirements needs to be achieved. Moreover, because ITO usually requires additional technology to be patterned after its deposition on the substrate ahead of application as transparent conductive film, TCF fabricated by simultaneous conductive-layer forming and patterning on a flexible film is preferred.

Received: July 18, 2013
Accepted: December 31, 2013
Published: December 31, 2013

   dx.doi.org/10.1021/am402900u | *ACS Appl. Mater. Interfaces* 2014, 6, 1447−1453

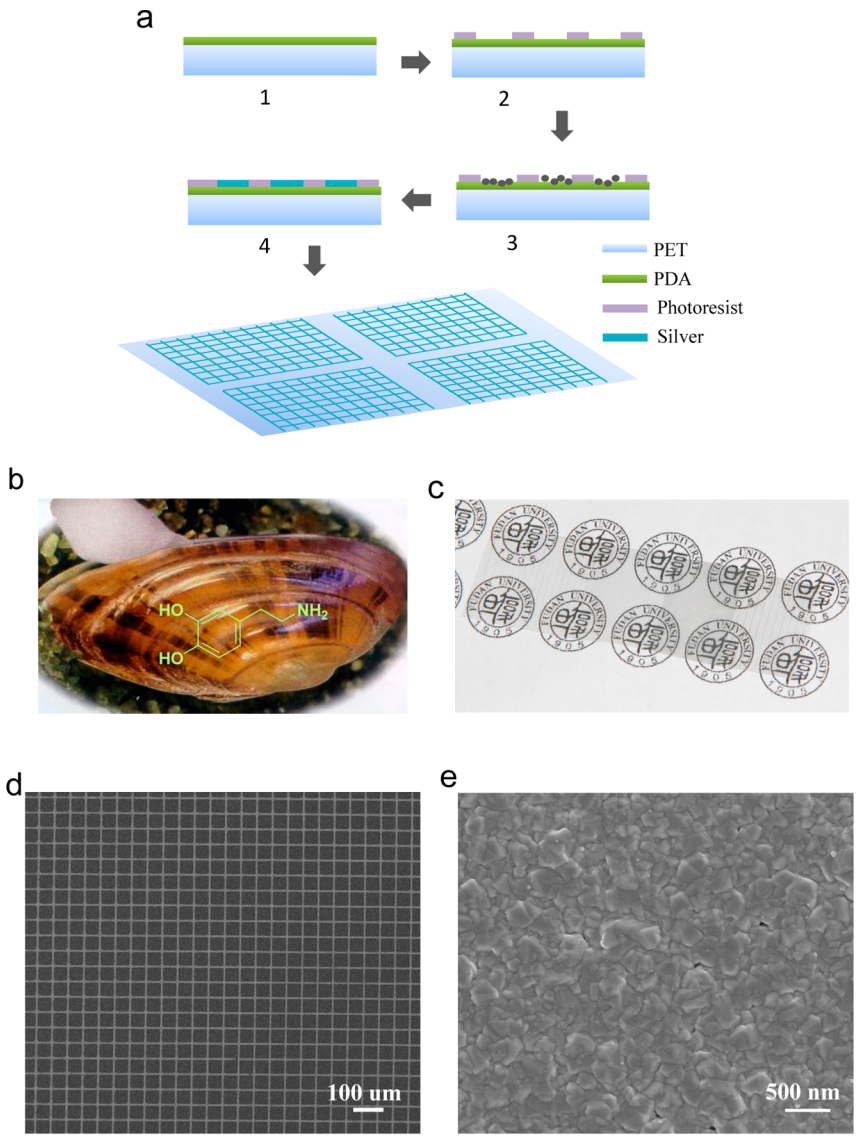

Figure 1. (a) Schematic illustration of the procedure for fabricating highly conductive silver grid film. (b) Mussel. The inset shows the chemical structure of dopamine inspired from mussel. (c) A photograph of the resultant transparent silver grids on PET. (d and e) SEM images of the silver grids.

In this report, we develop a versatile site-selective electroless plating approach through poly(dopamine) (PDA) surface-modification to fabricate silver grid films on polyethylene terephthalate (PET) as the flexible transparent conductive film. All the processes were conducted at room temperature, enabling the application of any heat-sensitive flexible materials as substrates and, of course, were energy efficient. Because electroless plating, one of the leading technologies for microelectronics metallization, was used, it is possible to provide the maximum conductivity of metal line compared with above fabrication methods due to the minimum contact resistance. Moreover, because of the exceptional adhesion properties even on wet surfaces,[19,20] PDA coating provided good adhesion to the silver grid film. In addition, due to the versatile deposition of poly(dopamine) on varied materials, using this method, a series of materials, rigid or flexible, hydrophobic or hydrophilic, organic or inorganic substance all can be used as the substrate. Most importantly, the silver grid formation and its pattering on PET was conducted in one step without additional processing, as required by ITO. As expected, the resultant silver grids films exhibit not only an extremely high σ_{DC}/σ_{Op} value in the range of 350−1000, but also particularly strong adhesion to the flexible substrate, which can resist ultrasonic treatment in water or organic solvent for several hours. A stable reliability for at least 1440 h of 85 °C/85% RH aging is also obtained.

EXPERIMENTAL SECTION

The fabrication process of patterned transparent conductive silver grid film is schematically illustrated in Figure 1a. After ultrasonic cleaning in ethanol, acetone, and deionized water, the PET sheet was dipped into a dopamine solution (Aladdin Reagent Co.) (2 mg mL^{-1} in 10 mM Tris−HCl buffer, pH = 8.5) at room temperature for 10−20 min (the structure of dopamine is shown in Figure 1b). The dopamine was oxidatively self-polymerized to poly(dopamine) at marine pH condition and deposited on the substrates (step 1). After rinsing with water and drying at 60 °C, a versatile photolithography process was conducted to form a PDA pattern as follows. Photoresist (Suzhou Ruihong Electronic Chemicals Co. Ltd.), sensitive to ultraviolet light,

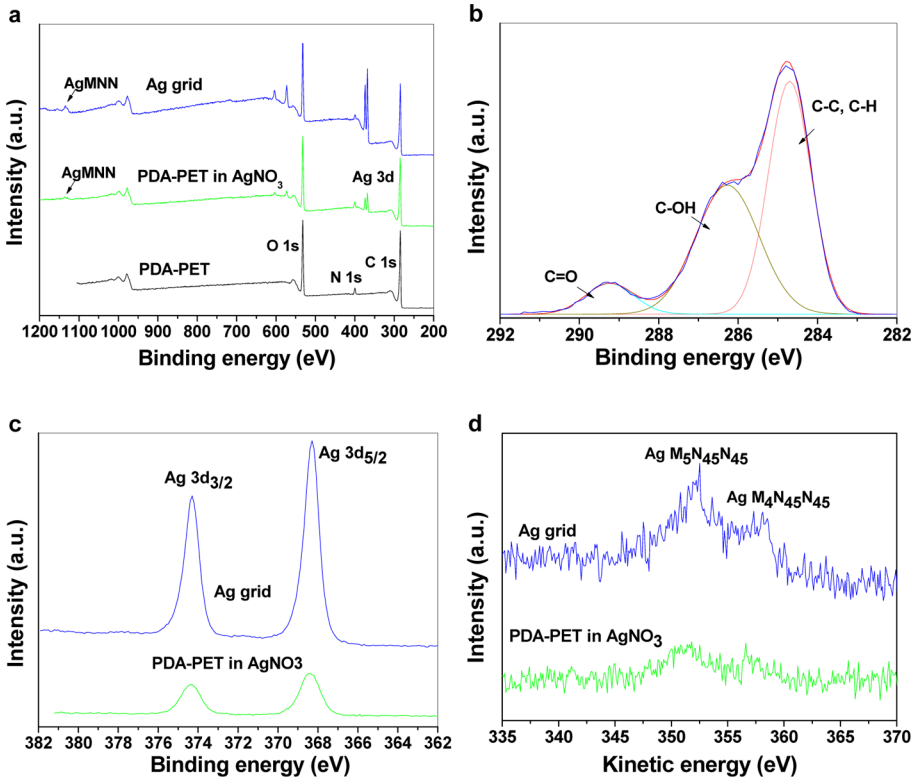

Figure 2. (a) Wide-scan XPS spectrum for PDA coated PET (PDA-PET), PDA coated PET immersion in silver nitrate ammonia solution for 5 min (PDA-PET in $AgNO_3$) and the resultant silver grid film (Ag grid). (b) Narrow-scan XPS spectra for C 1s of PDA-PET. (c) High resolution of Ag 3d spectrum. (d) The corresponding Ag MNN.

was coated on the PDA modified PET. After exposure to light through a metal photomask containning 10 kinds of grid sizes, the photoresist under the nonmetallized areas of a grid in the photomask became soluble and then was removed by the developer, yielding a PDA pattern in accordance with the layout of the photomask (step 2). The as-prepared PET was placed in a silver−ammonia solution (0.8−1 wt %) for 5 min (step 3). Then tartaric acid and NaOH were quickly added with a concentration of 0.8−1.2 wt % and 0.7−1.0 wt % in the final solution, respectively. After another 0.5 h, PET was taken out and washed with water and ethanol to remove the unexposed photoresist and other residuals. At last, silver was site-selectively electroless plated only on the exposed PDA arrays to form silver grids (step 4).

SEM images were obtained with a 6701F field emission scanning electron microscope (FE-SEM, JEOL). XPS analysis was carried out on a Kratos axis ultra DLD electron spectrometer from VG Scientific. Al Kα radiation was used as the X-ray source and operated at 300 W. UV−vis spectra were obtained by a T6 new century spectrophotometer (PGeneral) with the original PET substrate as a reference. The thicknesses of silver grids were measured using Surfcorder 300 surface profiler whose measuring range must be less than 1 μm. Adhesive strength between the silver grid and substrate was evaluated by testing according to the American Society for Testing and Materials (ASTM D3359). The adhesion was also investigated by a tape test in which a 12 mm wide 3M scotch tape was used to attach onto the silver grid film and then peeled off from the sample. The test was repeated for five times using a new tape for every test. The residue of silver grid after the test was observed with a microscope (Olympus BX51M). The I−V curve of the grid film was recorded by Keithley 2400 sourcemeter. Sheet resistance of the silver grid was measured by a four probe technique and calculated by the following equation:

$$R_s = \frac{\pi}{\ln 2} \times \frac{V}{I}$$

where V is the voltage and I is the current of the sample.

RESULTS AND DISCUSSION

Figure 1c shows the photograph of resultant silver grid patterns on PET. The darker area indicates the silver grid possessing a larger siver line width or smaller grid pitch. Their morphologies were further detected by SEM. As shown in Figure 1d, periodic two-dimensional silver grids with clear line edges were successfully fabricated. The enlarged SEM image (Figure 1e) shows the high quality of the individual silver line, exhibiting a dense and uniform surface, which enables the possibility of excellent conductivity performance of the grid film. The width and pitch of the silver grid was as low as several micrometers or lower, which was controlled by the patterning process, such as the grid size in photomask and the exposure parameter.

The XPS spectra and the Auger MNN spectra are shown in Figure 2, which verify the fabrication process. All the binding energies (BE) were corrected according to the C 1s that should be centered at 284.8 eV. C 1s, N 1s, and O 1s peaks are detected in the XPS curve of PET after dipping in an alkali dopamine solution (PDA-PET), confirming the formation of poly(dopamine) on the PET substrate. Figure 2b shows the narrow scan XPS spectrum and curve fitting of C 1s of PDA-PET. It results in three peaks at 289.0, 286.3, and 284.6 eV, which are assigned to C═O, C—OH and C—H, C—C, respectively. The C═O peak is associated with the substrate PET, suggesting that the thickness of the deposited poly(dopamine) is below the probing depth of the XPS technique (about 10 nm for organic matrix). Two characteristic Ag 3d peaks at 368.4 and 374.4 eV at high resolution XPS spectra (Figure 2c) were observed when PDA-coated PET was immersed into silver nitrate solution, among which the first peak is associated with Ag $3d_{5/2}$ and the second one with Ag $3d_{3/2}$. At last, much stronger Ag 3d peaks at 368.3 and 374.3 eV

dx.doi.org/10.1021/am402900u | ACS Appl. Mater. Interfaces 2014, 6, 1447−1453

were detected in XPS of resulting sample. Because the photoelectron peak of Ag $3d_{5/2}$ can display two BE value for metal silver and silver oxides, the Auger parameter (AP) was used to further identify silver states, considering the increased accuracy than that of the binding energy of Ag $3d_{5/2}$. The Auger parameter was calculated as BE (Ag $3d_{5/2}$) + KE (Ag MNN), where KE is the Auger kinetic energy, whose spectra are shown in Figure 2d. The binding energy values of Ag 3d and the Auger parameters are listed in Table 1. The PDA coated PET in silver nitrate and the Ag grid show AP value at 725.9 and 726.3 eV, respectively. In literature, the reported AP of metallic silver is 725.8−726.3 eV and that of silver ion is 724.0 eV.[21,22] The AP values here demonstrated the distinguishing reduced form Ag^0 from the oxidized form for the PDA coated PET in silver nitrate and the resultant Ag grid. Besides, the corresponding SEM image (Figure 3b) of PDA coated PET immersion in $AgNO_3$ exhibited isolated nanoparticles, whereas it showed a smooth surface before contact with silver ions. This suggests the successful formation of a seed layer of Ag nanoparticles. Moreover, the XPS result is also consistent with the SEM results in Figure 1d and e confirming the formation of silver grids.

Table 1. XPS Ag 3d characteristic peaks and the Auger parameters

	BE (eV)			
	Ag $3d_{5/2}$	Ag $3d_{3/2}$	KE (eV)	AP (eV)
PDA-PET in AgNO3	368.4	374.4	357.5	725.9
Ag grid	368.3	374.3	358.0	726.3

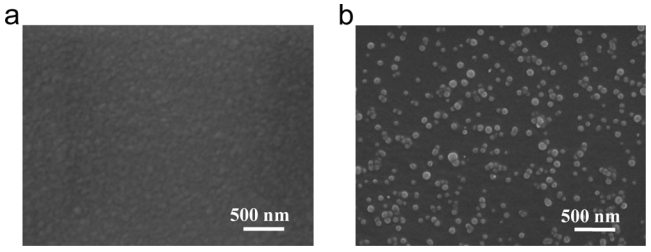

Figure 3. SEM images of (a) PDA coated PET by dipping PET in dopamine solution for 10 min. (b) The as-prepared PDA-coated PET immersion in silver nitrate ammonia solution for 5 min.

The selectivity of silver deposition, which only grows on the exposed PDA region, is a key and crucial process. Investigations indicated that a functional group, catechol, plays a decisive role in the exceptional wetness-resistant adhesion. Moreover, this group can also act as a reducing agent.[23] The fascinating properties of PDA allow us to use it simultaneously as an adhesive layer deposited on a PET substrate and as a reducing agent to transfer Ag^+ to Ag nanoparticles, which can serve as a seed layer during the electroless plating. Therefore, the patterned PDA on PET possibly enables the silver grid to grow site-selectively.

When tartaric acid was used as the reducing agent, the selectivity of silver deposition was good for the electroless bath exposure for near 1 h. While glucose was used, the selectivity of silver deposition was reduced after just several minutes or less. The reducing agent type also shows an intense relationship with the thicknesses of the silver grid lines. A typical thickness of 250 nm was observed when tartaric acid was used (Figure 4a). It kept constant with diverse PDA thickness on PET in terms of enough plating time. When glucose was used, the height always remained near 150 nm (Figure 4b). This may be due to the weak autocatalytic ability of metallic Ag.[24] Therefore, the thickness of a prepared silver line is possibly most reliant on the type of reducing agent in the case of no additional catalyst. This will offer a certain advantage of repeated uniform height of the silver grid on a large scale. Specifically, the sheet resistance of transparent metal grid electrode has been demonstrated to be reduced by a factor of 3 when the metal thickness is doubled.[15,17] Therefore, the uniform thickness here guarantees the homogeneous conductivity across the whole silver grid film.

Figure 5a shows the transmittance of silver grid films on a PET substrate. The transmittance keeps flat in the whole visible region. And, as designed, the transmittance was tuned over a large value with the aperture ratio, the area ratio of substrate that light can pass through, which is controlled by grid width and pitch. From these spectra, the transmittance at 550 nm, T, and sheet resistance, R_s, for all the films studied in this work were measured, as shown in Figure 5b. It exhibited far superior optical transmittance and electrical conductivity than other reported transparent conductors. The sheet resistance reaches 8.2 Ohm sq^{-1} for $T \sim 91.1\%$ and 27.4 Ohm sq^{-1} for $T \sim 95.9\%$.

Generally, performance of a transparent conductor is simply determined by a figure of merit of σ_{DC}/σ_{Op} value, which is calculated by eq 1 and quoted at $\lambda = 550$ nm.[25] This expression

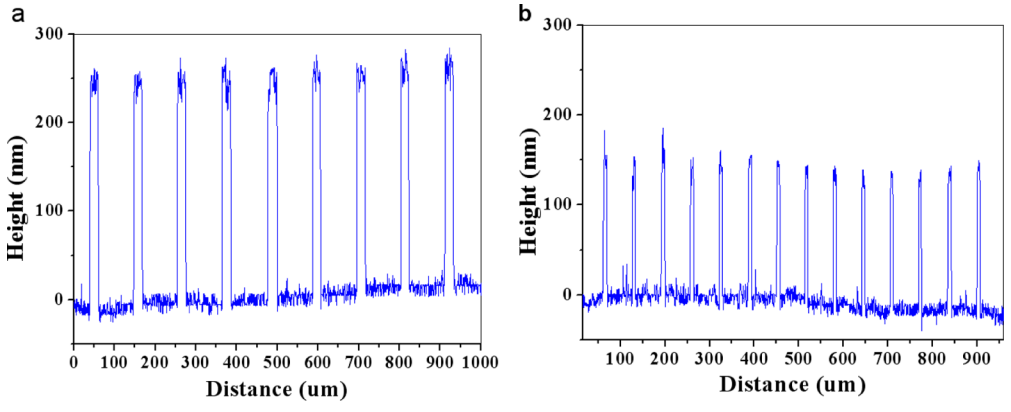

Figure 4. Typical line profiles of Ag grids with (a) tartaric acid and (b) glucose as the reducing agents.

dx.doi.org/10.1021/am402900u | ACS Appl. Mater. Interfaces 2014, 6, 1447−1453

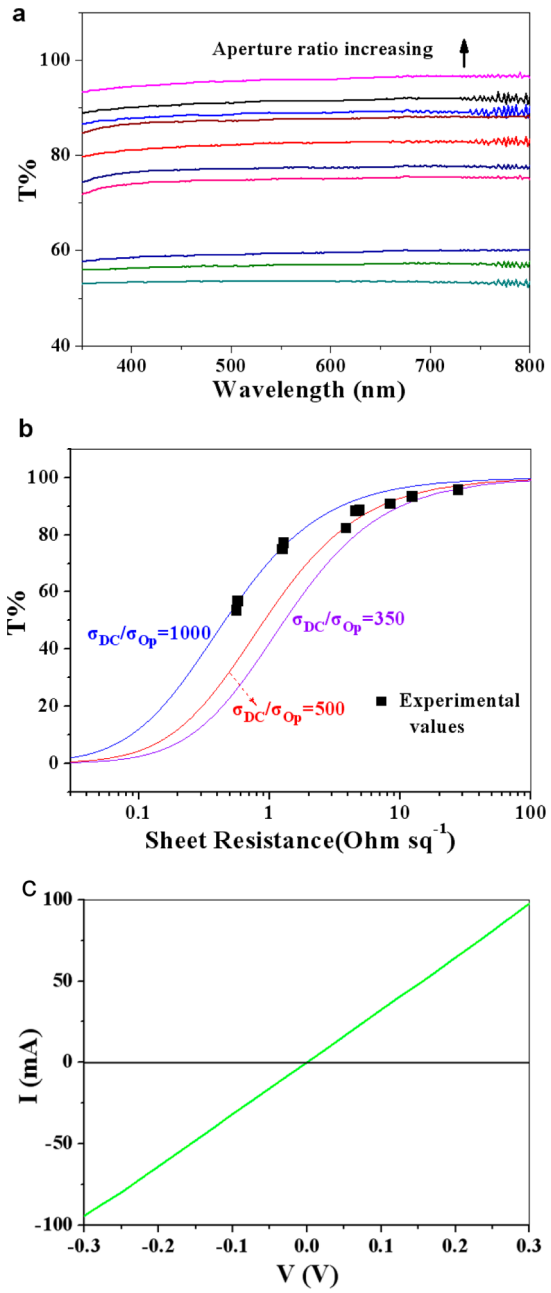

Figure 5. (a) Optical transmittance spectra for selected silver grid films with varied line width and pitch. (b) Optical transmittance (λ = 550 nm) plotted as a function of sheet resistance for films deposited on PET. The corresponding fits to eq 1 by using σDC/σOp of 1000, 500, and 350 are plotted as solid lines. (c) Current/voltage curve recorded for a grid film with length of 1.3 mm and width of 1 mm, underscoring high electric conductivity.

has been widely used by other workers and previously been shown to accurately describe films of carbon nanotubes.[26,27]

$$T(\lambda) = \left(1 + \frac{188.5}{R_s}\frac{\sigma_{Op}(\lambda)}{\sigma_{DC}}\right)^{-2} \quad (1)$$

This expression has been fitted to the data in Figure 5b using three different values of σ_{DC}/σ_{Op} = 1000, 500, and 350 (solid lines). The optimum value of σ_{DC}/σ_{Op} approached as high as 1000 for $T \sim 77\%$. This value is extremely large for a transparent electrode. We note that this transmittance sheet resistance result is far superior to that found in the literature for TCFs. Generally, the transmittance in the visible light range of at least 80% is necessary to function with present electronic devices requirements. Therefore, the value of σ_{DC}/σ_{Op} at high transmittance is particularly important. The fit to eq 1 shown in Figure 5b is described by σ_{DC}/σ_{Op} near 500 in the range of $T \sim$ 82%−94% and 350 even for $T \sim 96\%$, which is superior to other reported transparent conductors from CNTs, graphene,[7−10] ITOs,[17] and Ag NWs.[12−14] Similarly, an excellent conductivity profile for grid film is also apparently demonstrated in Figure 5c, indicating electron transport through the silver grid under a low voltage. To further verify the electrical performance, the resistivity of single silver line with width of 1.5 mm was investigated. It is noted that the resistivity was as low as 5.0−7.4 $\mu\Omega$·cm, which is about 3−5 times of the resistivity of the pure silver. Therefore, we attribute the excellent conductivity of the fabricated silver grid to the low resistivity of the silver line and the low contact resistance among grids.

To be used in optoelectronic devices, especially the flexible devices, transparent electrodes must fulfill certain mechanical requirements to ensure device reliability. An adhesion test according to the American Society for Testing and Materials (ASTM D3359) was utilized to assess the adhesive strength between the silver grids and the PET substrate, in which ASTM 5B and 0B represent the best and the worst adhesion grade, respectively. Figure 6a shows the samples after the test. All the samples exhibited excellent adhesion properties of grade 5B. We also studied the adhesion by measuring sheet resistance and transmittance of silver grid after the tape test. As revealed in Figure 6b, the R_s and T exhibited nearly no difference after five tape tests.

Moreover, we further test the adhesive strength by measuring the sheet resistance of Ag grid film against water and acetone exposure, which are standard tests used in manufacturing.[28] The sheet resistance is 1.4 times the original value after immersion in acetone up to 24 h, whereas in water, it becomes 2.4 times (Figure 6c). The R_s rise may be due to the oxidation of silver grids in the solvent. The two samples both still show adhesion grade of 5B after immersion in the solvent for 24 h. Thus, we further inspected the adhesive strength by an accelerated test, in which ultrasonic shock with a power of 300 W and a frequency of 40 kHz was loaded to the samples when they were placed in the solvent. The sheet resistance shows almost no change after 5 h of ultrasonication in acetone, and exfoliation of the silver grid was not observed. While in water, very little of the silver grid exfoliated from the PET substrate after 1.5 h of ultrasonication. The slightly weaker adhesion may be due to the presence of trace ions in the water, which can reduce the adhesion of PDA on the substrate.[29] Furthermore, we continue to investigate the adhesion and reliability by measuring the sheet resistance during a long-term temperature−humidity testing (THT) (Figure 7). During two months of 85 °C/85% RH aging, the sheet resistance remained effectively flat, with a minor decrease in the early stage of the test. It is possible that the electrical contacts inside the silver line are improved due to the heating. In short, all the results revealed the outstanding stability of silver grids on PET's resistance to solvent and long-term hygrothermal aging.

Besides the high electrical conductivity in the static state, TCFs for flexible electronics need to maintain their conductivity under mechanical deformation. Thus, the flexibility of TCF is another significant requirement. We measured the sheet resistance over repeated bending cycles

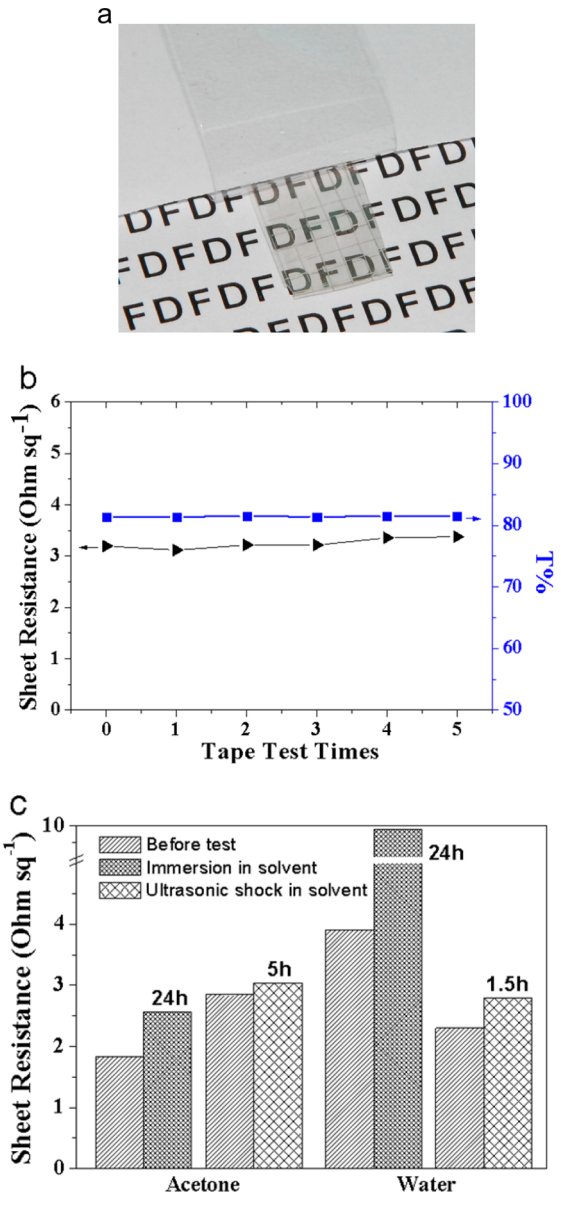

Figure 6. (a) Adhesive test result of the silver grid film on PET substrate according to ASTM D3359. (b) Sheet resistance and transmittance as a function of cycles of tape test. (c) The sheet resistance variations of Ag grid film after exposure to acetone and water.

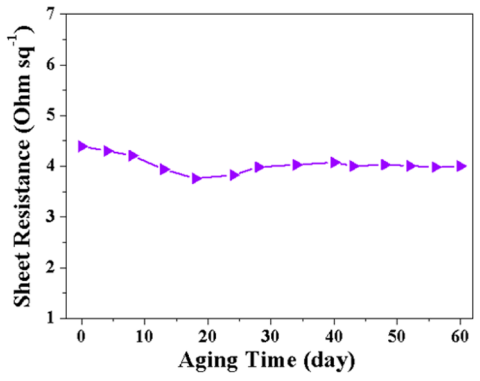

Figure 7. Sheet resistance of Ag grid film during temperature–humidity test versus aging time.

under a bending radius of 3 mm. As shown in Figure 8a, the sheet resistance only changes less than 10% over the whole

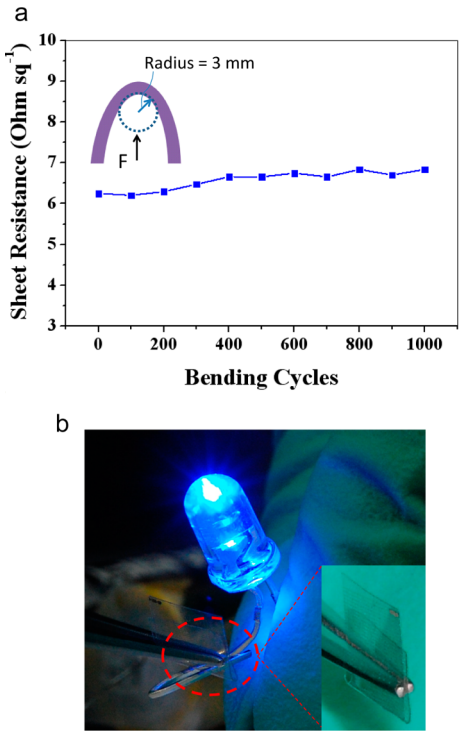

Figure 8. (a) Sheet resistance change of Ag grid film during 1000 bending cycles (3 mm bending radius). Inset is the schematic illustration of the bent state. (b) A photographic image of a circuit containing a near 180° folded Ag grid film, which connects to an LED light. The LED becomes blue when the circuit is on. The inset is photograph of the folding state of Ag grid film.

1000 cycles. The standard specification for the change in the sheet resistance should be less than 30%, and varies for different device applications and companies.[30] The conductivity in the bent state of the silver grid film was further studied. As shown in Figure 8b, a circuit composed of a folded Ag grid film (held by a clamp close to a 180° fold), an LED and a battery was fabricated. When the pin of the LED was anchored just right on the folding position of the Ag grid film, the LED lit up for a long time, indicating the good conductivity of fabricated Ag grid film under the heavy folded status.

CONCLUSIONS

In conclusion, we fabricated a transparent conductive Ag grid film on a flexible PET substrate via a facile approach. Conductive Ag grid film forming and patterning on PET was carried out simultaneously. The investigation suggests that poly(dopamine) plays a critical role during the process, providing good adhesion and site-selective growth of the silver grid. The sheet resistance for $T \sim 91.1\%$ is less than 10 Ohm sq^{-1}. The σ_{DC}/σ_{Op} values are bigger than 350 at high transmittance, and up to maximum 1000. The resulting Ag grid film shows outstanding stability and resistance to solvent and long-term hygrothermal aging. After 1000 bending cycles the sheet resistance changes less than 10%. We believe that such films with great comprehensive performance hold great promise as flexible transparent electrodes for flexible electronics.

AUTHOR INFORMATION

Corresponding Author

*F. Xiao. Phone: +86-21-65642110. E-mail: feixiao@fudan.edu.cn.

Notes

The authors declare no competing financial interest.

ACKNOWLEDGMENTS

This study was supported by National Science and Technology Major Project with Contract nos. 2011ZX02602 and 2013ZX02505.

REFERENCES

(1) Hu, L.; Wu, H.; Cui, Y. *MRS Bull.* **2011**, *36*, 760−765.
(2) Lipomi, D. J.; Tee, B. C. K.; Vosgueritchian, M.; Bao, Z. *Adv. Mater.* **2011**, *23*, 1771−1775.
(3) Layani, M.; Magdassi, S. *J. Mater. Chem.* **2011**, *21*, 15378−15382.
(4) Kumar, A.; Zhou, C. *ACS Nano* **2010**, *4*, 11−14.
(5) Yang, L.; Zhang, T.; Zhou, H.; Price, S. C.; Wiley, B. J.; You, W. *ACS Appl. Mater. Interfaces* **2011**, *3*, 4075−4084.
(6) Hong, S.; Yeo, J.; Kim, G.; Kim, D.; Lee, H.; Kwon, J.; Lee, H.; Lee, P.; Ko, S. H. *ACS Nano* **2013**, *7*, 5024−5031.
(7) Hu, L.; Hecht, D.; Grüner, G. *Nano Lett.* **2004**, *4*, 2513−2517.
(8) Bae, S.; Kim, H.; Lee, Y.; Xu, X.; Park, J. S.; Zheng, Y.; Balakrishnan, J.; Lei, T.; Kim, H. R.; Song, Y. I. *Nat. Nanotechnol.* **2010**, *5*, 574−578.
(9) Chen, J.; Bi, H.; Sun, S.; Tang, Y.; Zhao, W.; Lin, T.; Wan, D.; Huang, F.; Zhou, X.; Xie, X.; Jiang, M. *ACS Appl. Mater. Interfaces* **2013**, *5*, 1408−1413.
(10) Geng, H. Z.; Lee, D. S.; Kim, K. K.; Han, G. H.; Park, H. K.; Lee, Y. H. *Chem. Phys. Lett.* **2008**, *455*, 275−278.
(11) De, S.; Higgins, T. M.; Lyons, P. E.; Doherty, E. M.; Nirmalraj, P. N.; Blau, W. J.; Boland, J. J.; Coleman, J. N. *ACS Nano* **2009**, *3*, 1767−1774.
(12) Hu, W.; Niu, X.; Li, L.; Yun, S.; Yu, Z.; Pei, Q. *Nanotechnology* **2012**, *23*, 344002−344011.
(13) Madaria, A. R.; Kumar, A.; Zhou, C. *Nanotechnology* **2011**, *22*, 245201−245208.
(14) Tokuno, T.; Nogi, M.; Karakawa, M.; Jiu, J.; Nge, T.; Aso, Y.; Suganuma, K. *Nano Res.* **2011**, *4*, 1215−1222.
(15) Kang, M. G.; Guo, L. J. *Adv. Mater.* **2007**, *19*, 1391−1396.
(16) Galagan, Y.; Rubingh, J. M.; Andriessen, R.; Fan, C. C.; Blom, W. M.; Veenstra, C. S.; Kroon, J. M. J. *Sol. Energy Mater. Sol. Cells* **2011**, *95*, 1339−1343.
(17) Kang, M. G.; Park, J. H.; Ahn, H. S.; Guo, J. L. *Sol. Energy Mater. Sol. Cells* **2010**, *94*, 1179−1184.
(18) Yu, J. S.; Jung, G. H.; Jo, J.; Kim, J. S.; Kim, J. W.; Kwak, S. W.; Lee, J. L.; Kim, I.; Kim, D. *Sol. Energy Mater. Sol. Cells* **2013**, *109*, 142−147.
(19) Ryou, M. H.; Kim, J.; Lee, I.; Kim, S.; Jeong, Y. K.; Hong, S.; Ryu, J. H.; Kim, T. S.; Park, J. K.; Lee, H.; Choi, J. W. *Adv. Mater.* **2013**, *25*, 1571−6.
(20) Brubaker, C. E.; Messersmith, P. B. *Langmuir* **2012**, *28*, 2200−2205.
(21) Machocki, A.; Avgouropoulos, G.; Machocki, A.; Avgouropoulos, G.; Ioannides, T.; Delimaris, D.; Stasinska, B.; Gac, W.; Grzegorczyk, W.; Pasieczna, S. *J. Catal.* **2004**, *227*, 282−296.
(22) Fonseca, A. M.; Neves, I. C. *Micropor. Mesopor. Mat.* **2013**, *181*, 83−87.
(23) Xu, L. Q.; Yang, W. J.; Neoh, K. G.; Kang, E. T.; Fu, G. D. *Macromolecules* **2010**, *43*, 8336−8339.
(24) Krulik, G. A. *Electroless Plating in Encyclopedia of Chemical Technology*, 4th ed.; John Wiley and Sons: New York, 1994; p 198.
(25) Dressel, M.; Gruner, G. *Electrodynamics of Solids: Optical Properties of Electrons in Matter*; Cambridge University Press: Cambridge, 2002.
(26) Geng, H. Z.; Lee, D. S.; Kim, K. K.; Han, G. H.; Park, H. K.; Lee, Y. H. *Chem. Phys. Lett.* **2008**, *455*, 275−278.
(27) De, S.; Lyons, P. E.; Sorel, S.; Doherty, E. M.; King, P. J.; Blau, W. J.; Nirmalraj, P. N.; Boland, J. J.; Scardaci, V.; Joimel, J. *ACS Nano* **2009**, *3*, 714−720.
(28) Hecht, D. S.; Thomas, D.; Hu, L.; Ladous, C.; Lam, T.; Park, Y.; Irvin, G.; Drzaic, P. *J. Soc. Inf. Disp.* **2012**, *17*, 941−946.
(29) Hwang, D. S.; Zeng, H.; Lu, Q.; Israelachvili, J.; Waite, J. H. *Soft Matter* **2012**, *8*, 5640−5648.
(30) Hu, L.; Kim, H. S.; Lee, J. Y.; Peumans, P.; Cui, Y. *ACS Nano* **2010**, *4*, 2955−2963.